SNe Ia: LC diagnostics Methods

Redshift evolution (Link to progenitor and system)
Interstellar reddening (separate intrinsic variation before RC).
Why do SN Ia look like M(Ch) but only in spherical models ?
Towards a fix of a deadly flaw.

1) Secondary LC Parameter

2) Spectroscopic tests

3) Bolometric light curves

4) New physical effects and tests
   using V and H light curves

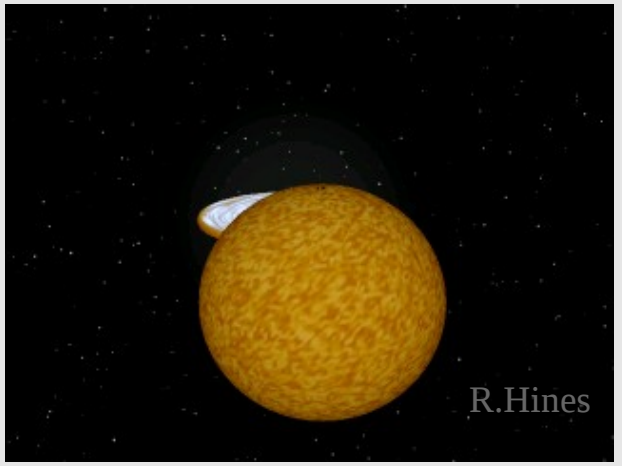

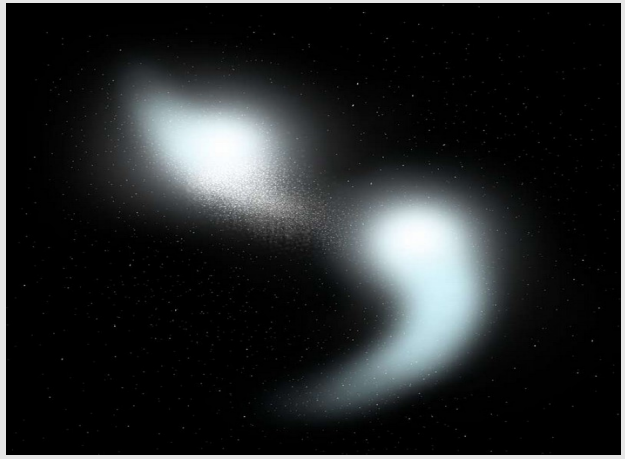

Example of a DD model (reminder)

[M(MS)= 3 Mo; Z = 1.E-3 solar; rho(c)= 2E9 g/ccm with rho(tr)=8, 16, 25 g/ccm]

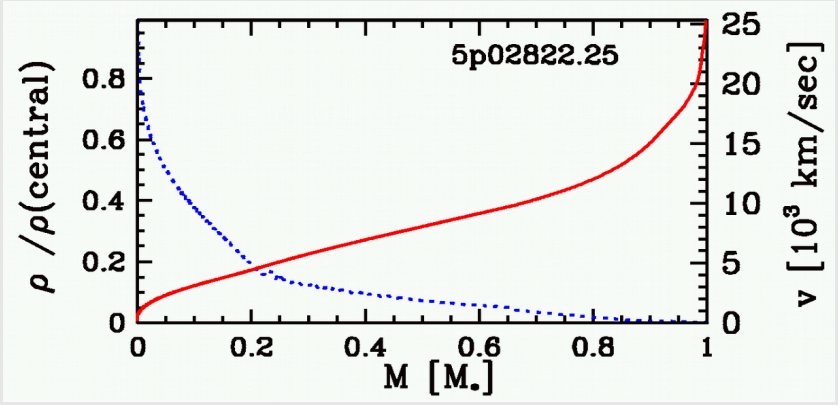

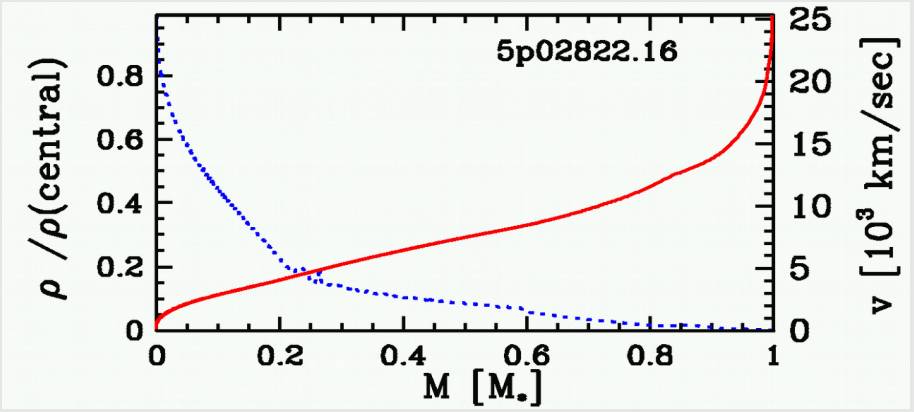

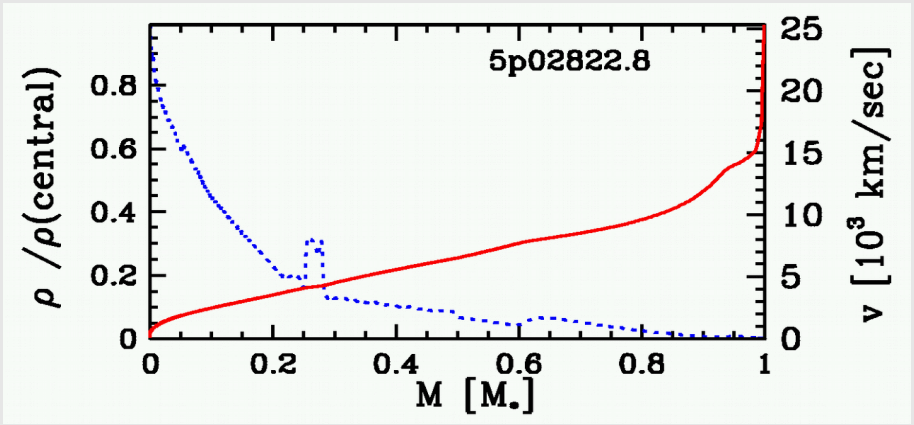

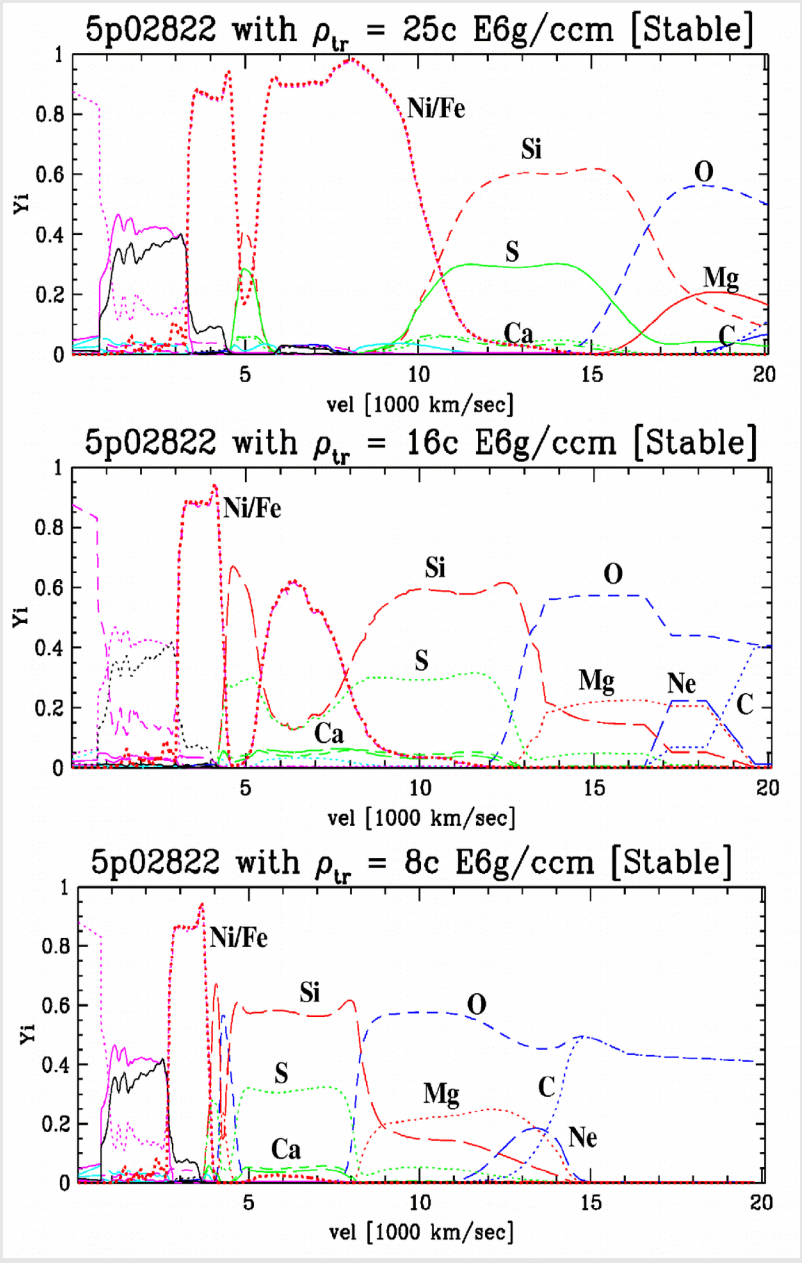

56Ni (deflagration phase) / 56Ni (total) ≃ 10 … 12

Comparison with Observations

The brightness decline relation and colors (Hoeflich et al. 1996, 2002)

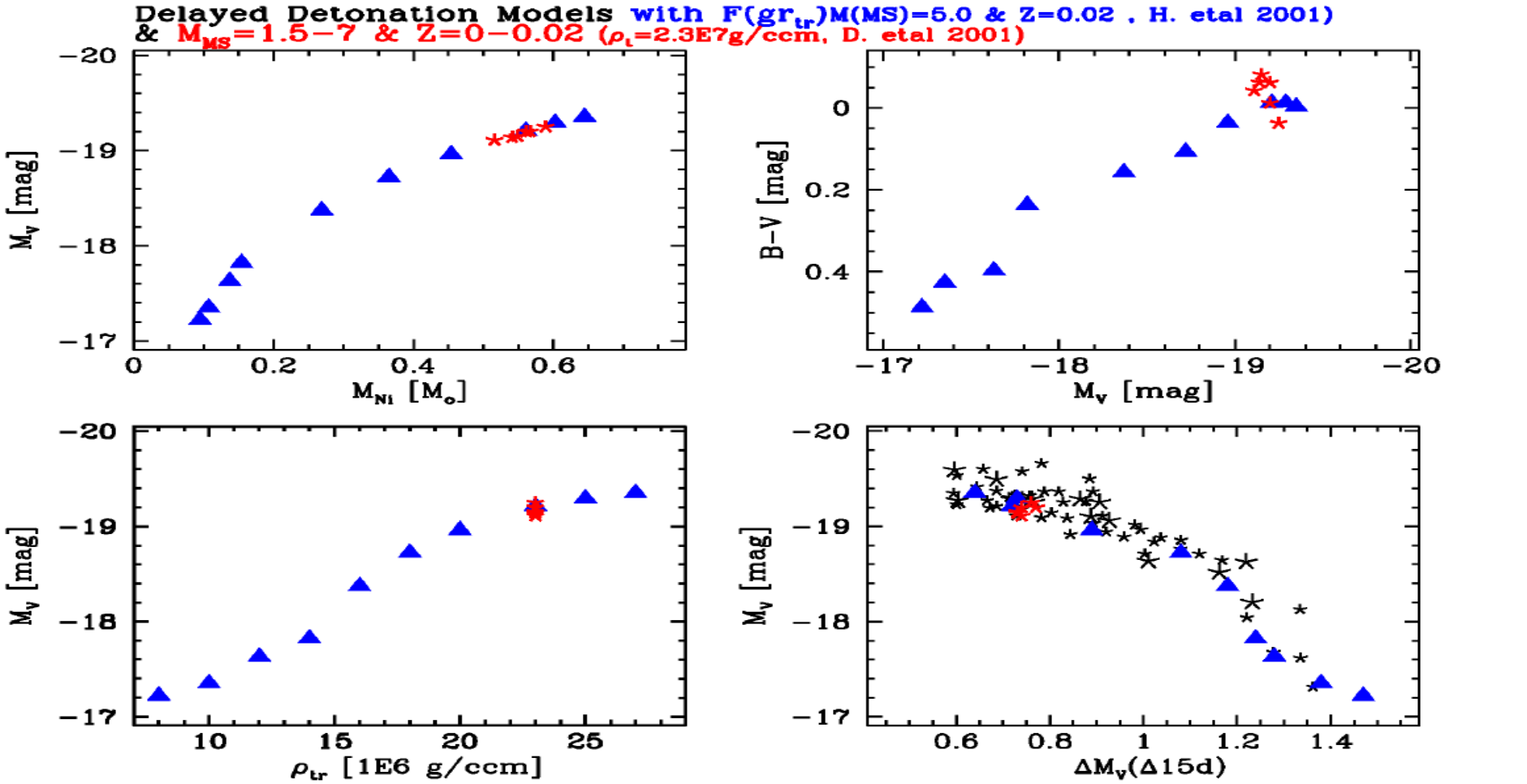

- **Generic: Brightness decline relation is an opacity effect** (Hoeflich etal 96,Mazzali et al. 2001,Kasen et al. 2009)
- **Small spread requires similar explosion energies** *(±0.5mag for all scenarios H. et al. 96)*
- **Within DD models, relation can be understood as change of burning before DDT**
- **Progenitors (Z=0 ... solar) can produce systematics of about 0.3 mag.**

Attention: Color change of about 0.2 mag -> reddening !!!

Progenitor Signatures in Differentials of SNIa pairs

Differential change light-curves after Stretch (Hoe

Observations (Fogliatti et a

C/O profile of the WD (explosion energy)
depends on MS mass
and metallicity of progenitor
(from Nomoto, Hetal01)

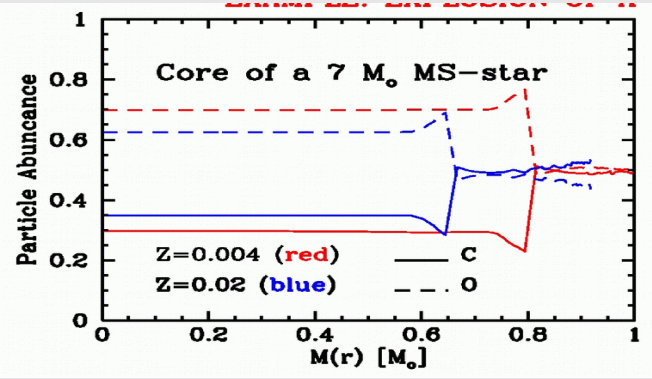

Theory (predicted, H.etal 98)

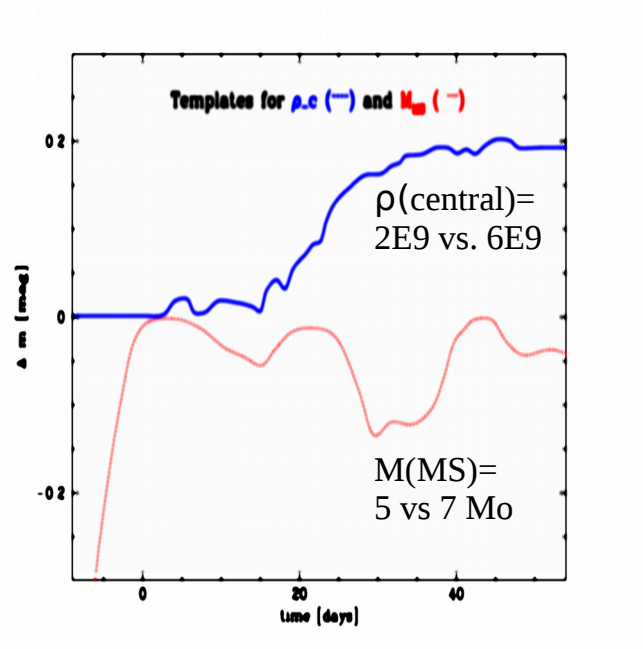

Accretion Rate =>

Central density at explosion
changes electron capture
(inner 56Ni contribution)
(H. et al 2006)

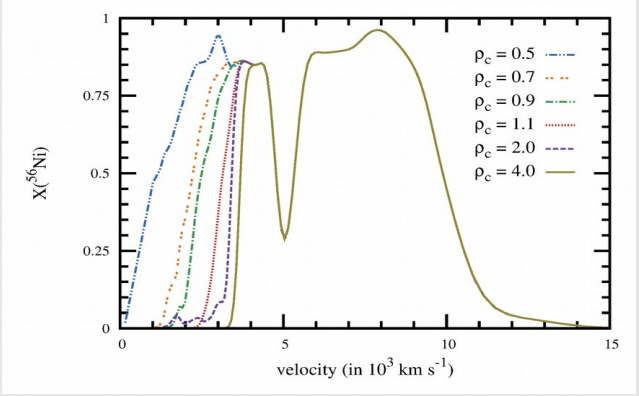

Progenitor Signatures in Differentials of SNIa pairs

Differential change light-curves after Stretch (Hoe

Observations (Fogliatti et a

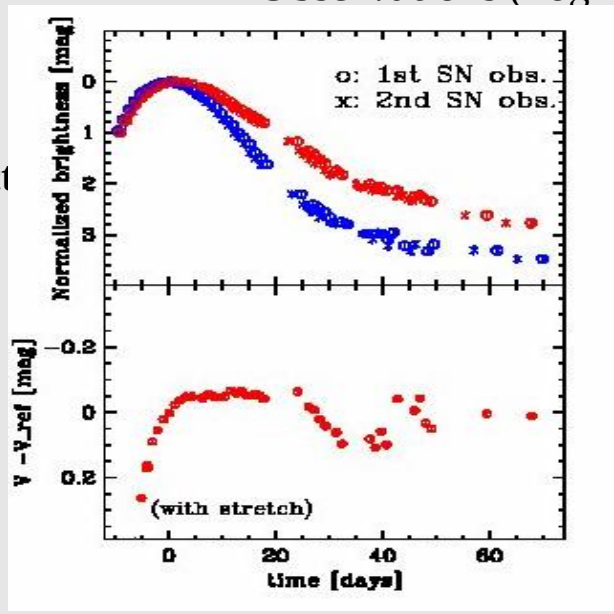

Theory (predict

C/O profile of the WD

depends on MS mass and metallicity of WD (from Nomoto, Hetal01)

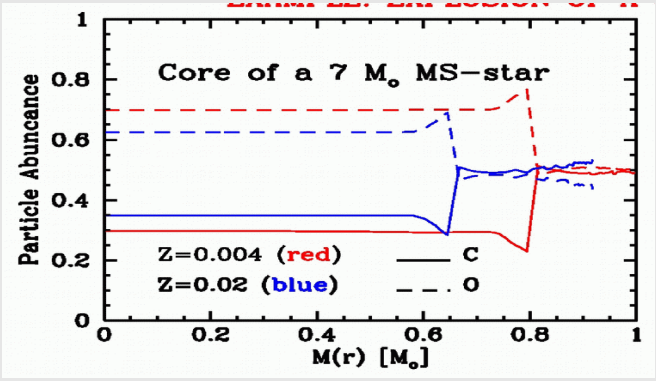

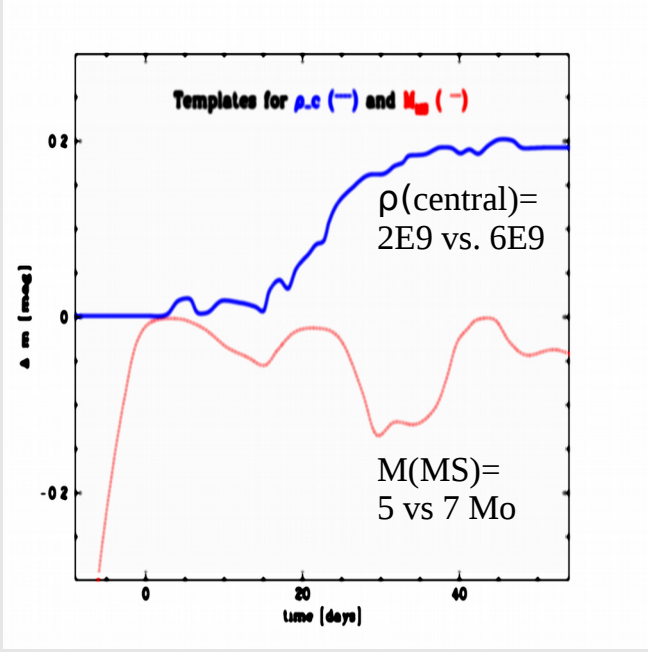

Accretion Rate =>

Central density at explosion changes electron capture (Hetal06) and 56Ni distribution

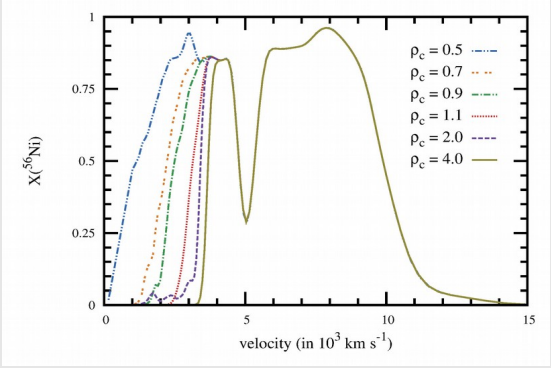

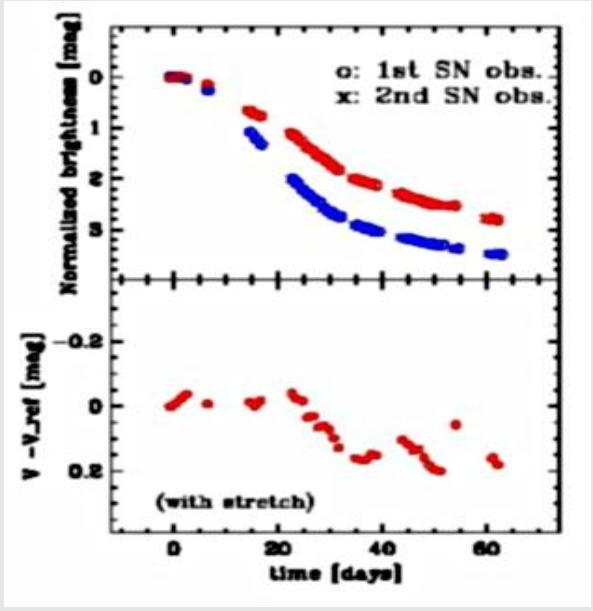

Examples from the CSP survey:

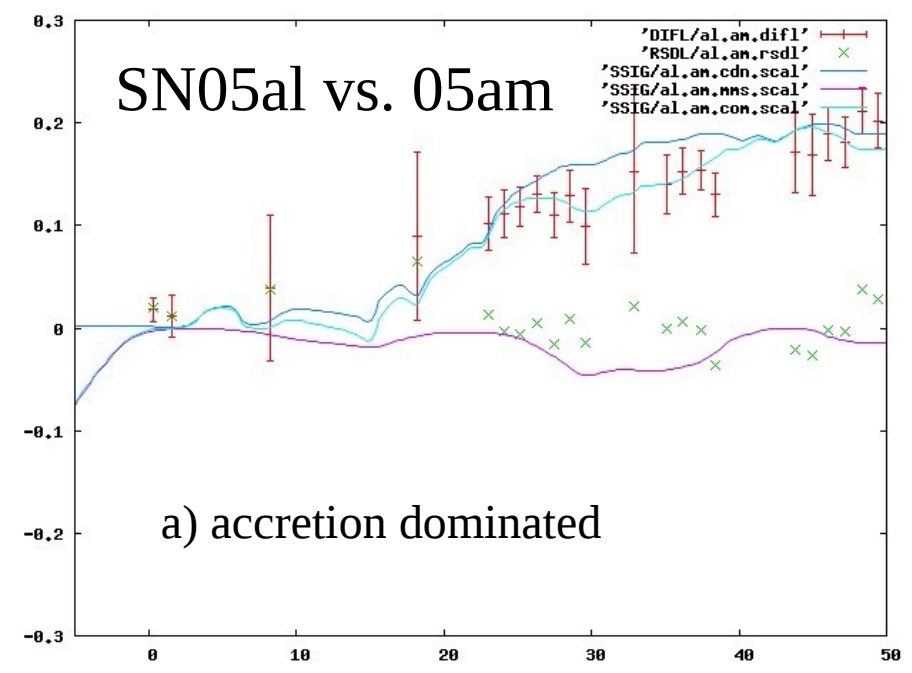

a) accretion dominated

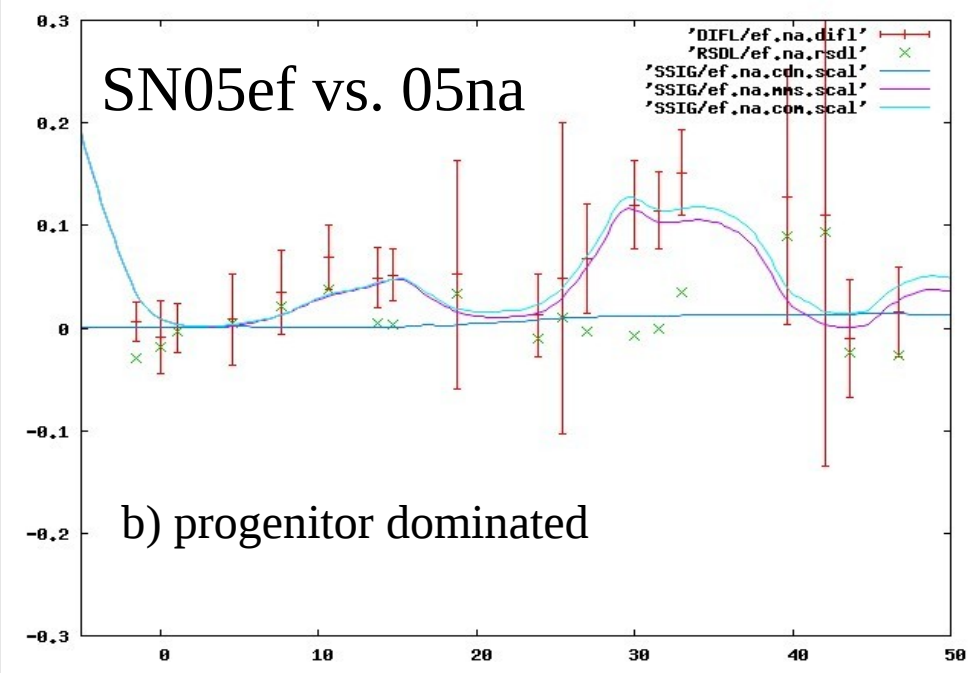

b) progenitor dominated

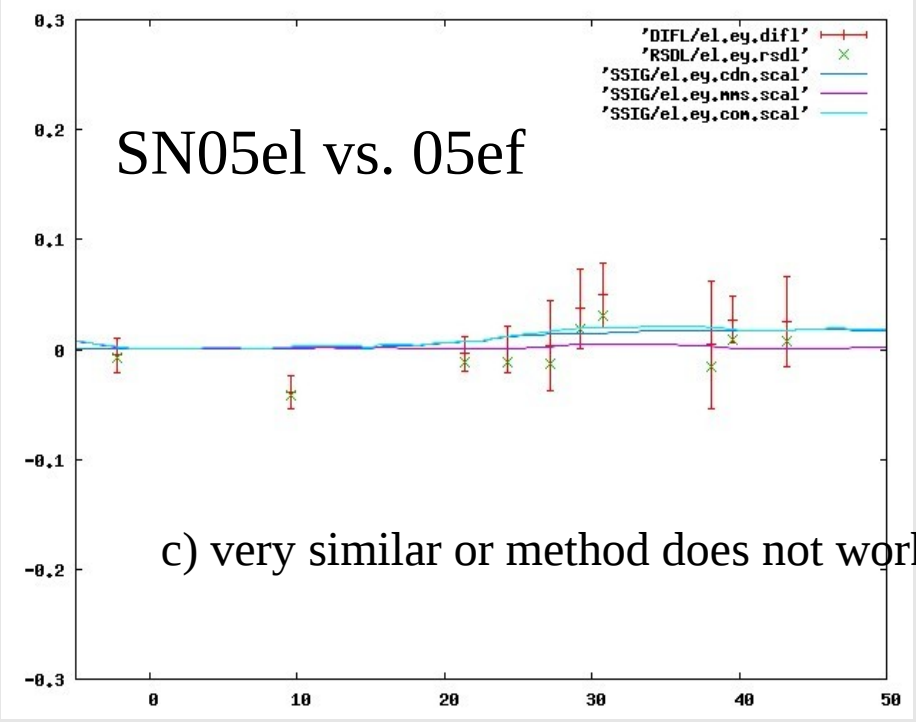

c) very similar or method does not work

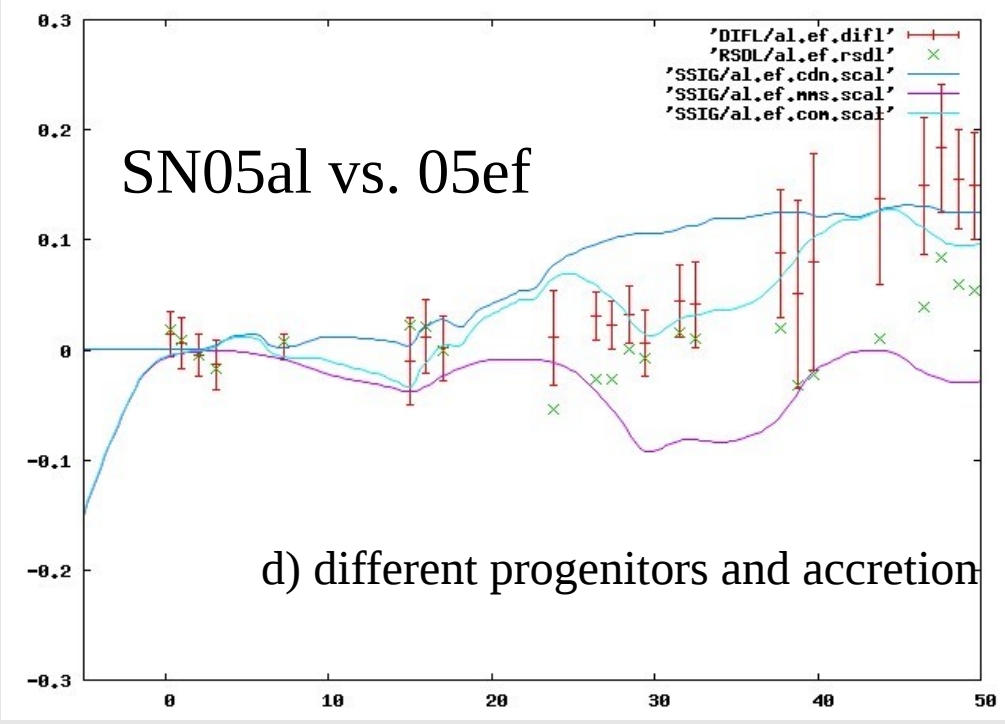

d) different progenitors and accretion

Fits of Actual SN-Pairs & Distribution for CSP

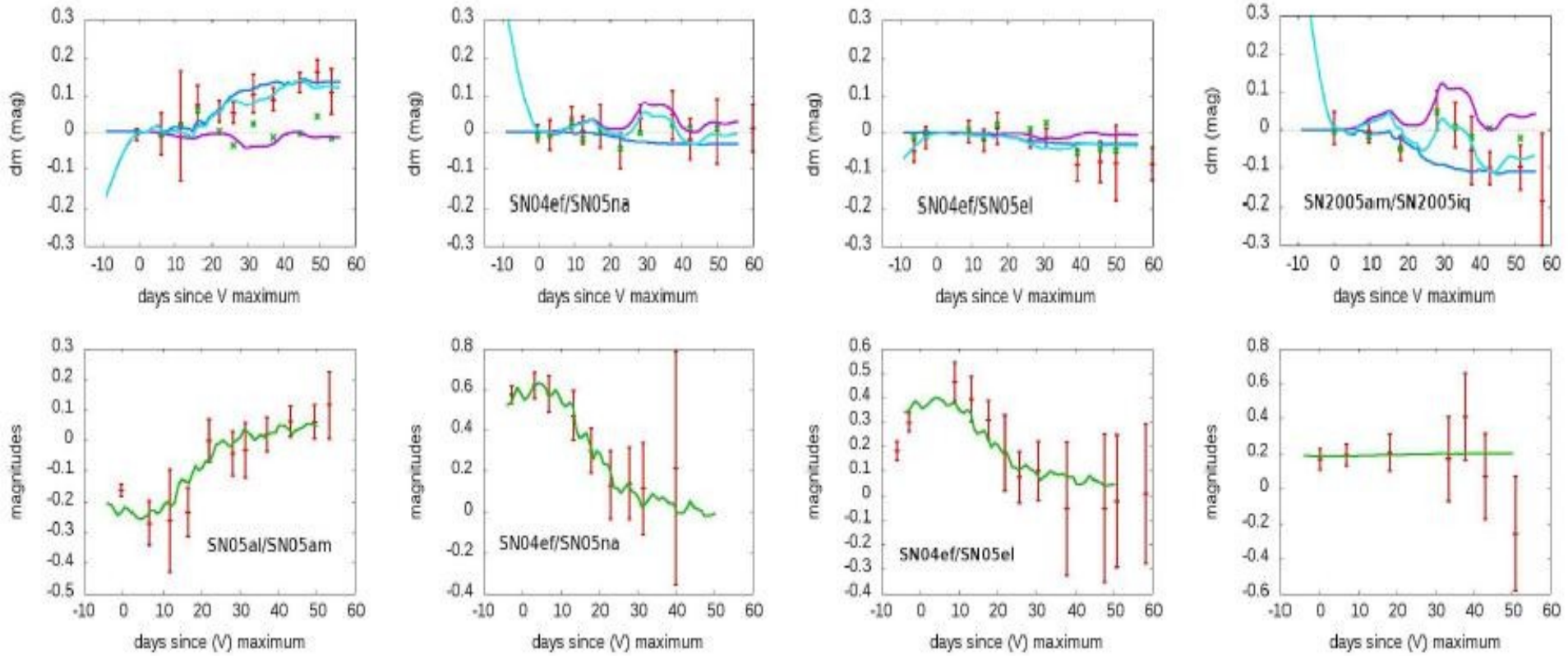

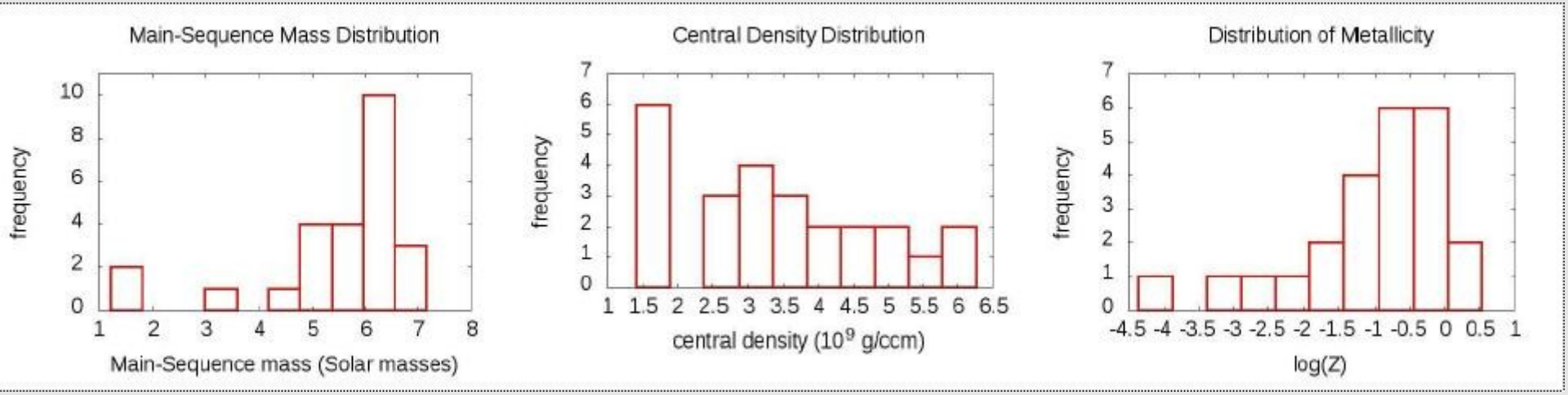

Next Break: MIR from the Ground for SN2014J

(Telesco et al. 2014)

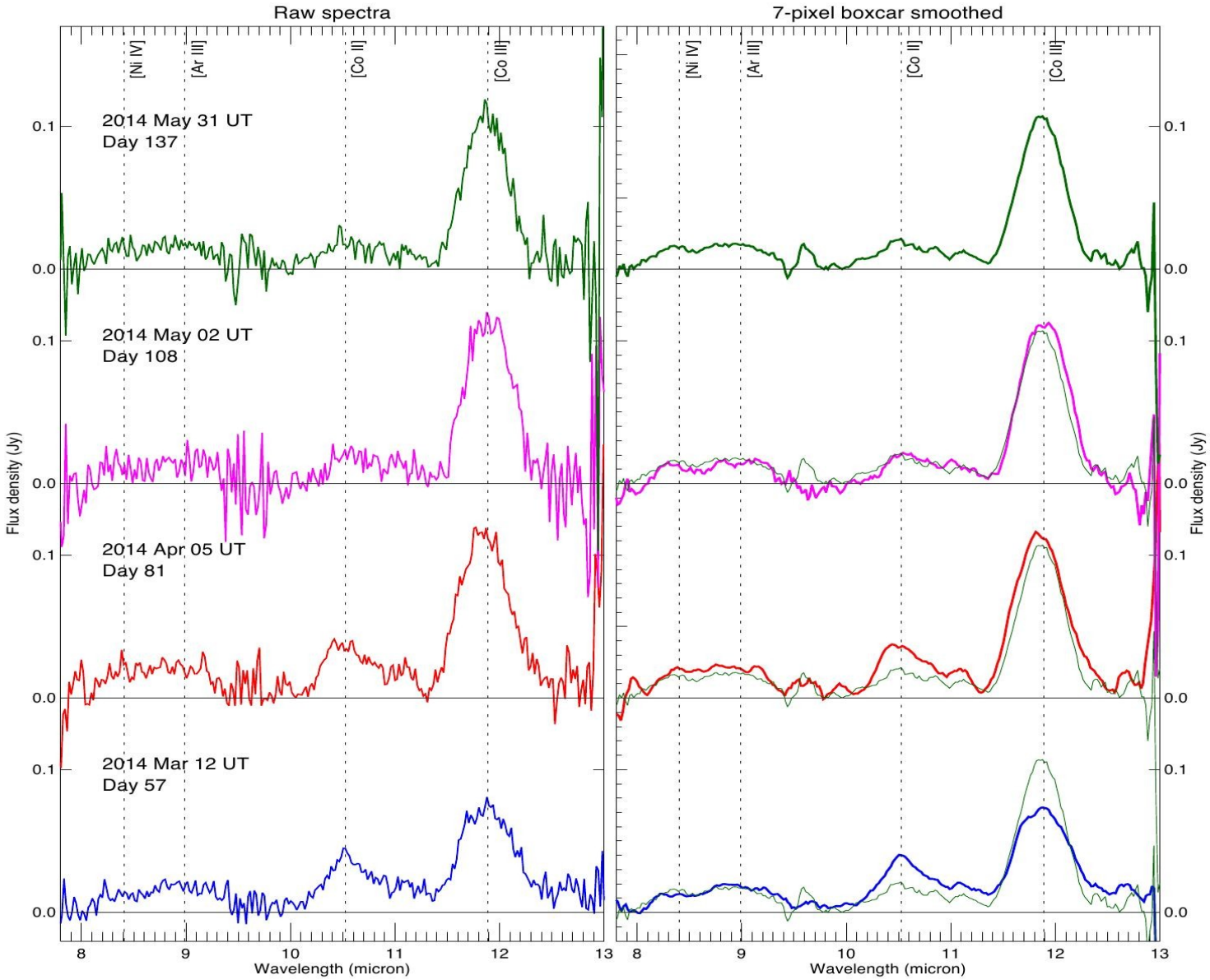

SN2014J compared to a DD models with 0.6 Mo (without tuning)

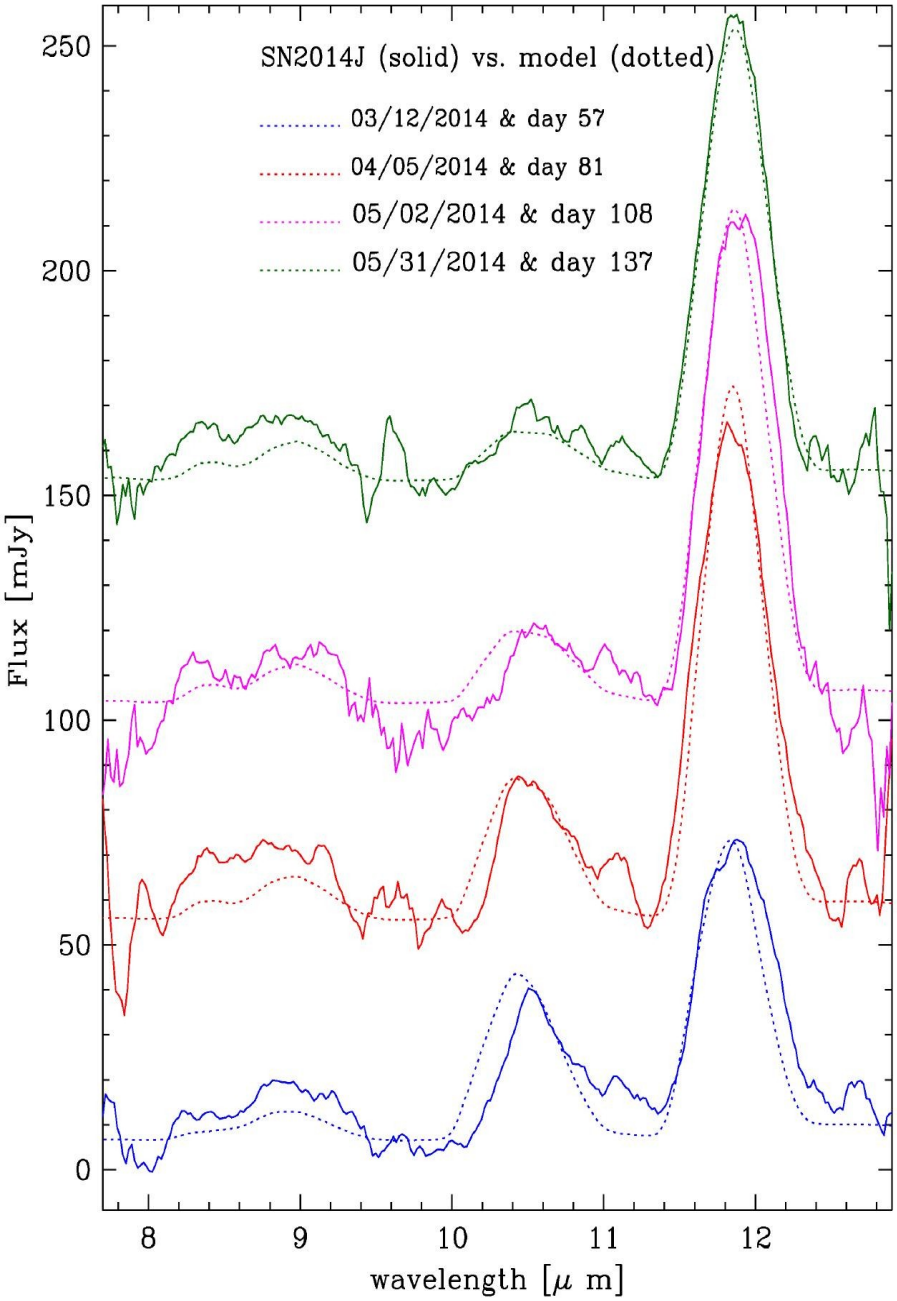

Table 2. Strong Mid-IR Forbidden Lines in Reference Model

λ [μm]	Str.	Ion	Configuration	Term	$J_{l,u}$	A_{ul}	$g_u A_{ul}$	$E_{l,u}$ [cm^{-1}]
7.791	++	[Fe III]	3d6-3d6	3P4-3P4	2-1	4.70E-02	1.41E-01	19404-20687
8.211	+	[Fe III]	3d6-3d6	3H-3F4	4-3	1.50E-08	1.05E-07	20481-21699
8.405	++	[Ni IV]	3d7-3d7	4F-4F	9/2-7/2	5.70E-02	4.56E-01	0-1189
8.611	+	[Fe III]	3d6-3d6	3H-3F4	5-4	9.50E-09	8.55E-08	20300-21462
8.991	++	[Ar III]	3s2.3p4-3s2.3p4	3P-3P	2-1	3.10E-02	9.30E-02	0-1112
9.723		[Ni IV]	3d7-3d7	2H-2H	11/2-9/2	1.60E-02	1.60E-01	26649-27677
9.975		[Ni IV]	3d7-3d7	2P-2P	3/2-1/2	1.70E-02	3.40E-02	23648-24651
10.080		[Ni II]	3d8.(1D).4s-3d8.(3P).4s	2D-4P	3/2-3/2	1.20E-02	4.80E-02	23796-24788
10.088		[Fe III]	3d6-3d6	1S4-1D4	0-2	8.10E-10	4.05E-09	34812-35803
10.203	+	[Fe III]	3d6-3d6	3H-3F4	4-4	1.60E-03	1.44E-02	20482-21462
10.523	++	[Co II]	3d8-3d8	a3F-a3F	4-3	2.23E-02	1.56E-01	0-950
10.682	+	[Ni II]	3d8.(3F).4s-3d8.(3F).4s	4F-4F	9/2-7/2	2.71E-02	2.17E-01	8394-9330
11.002		[Ni III]	3d8-3d8	3F-3F	3-2	2.70E-02	1.35E-01	1371-2270
11.167		[Co II]	3d7.(4F).4s-3d7.(4F).4s	b3F-b3F	4-3	1.87E-02	1.31E-01	9813-10708
11.726	++	[Ni IV]	3d7-3d7	4F-4F	7/2-5/2	3.60E-02	2.16E-01	1190-2043
11.888	+++	[Co III]	3d7-3d7	a4F-a4F	9/2-7/2	2.00E-02	1.60E-01	0-841
11.978		[Fe III]	3d6-3d6	3P2-3P2	1-2	7.90E-03	3.95E-02	49576.8-50412
12.641		[Fe II]	3d7-3d7	a2D2-a2D2	5/2-3/2	8.01E-03	3.20E-02	20517-21308
12.681	+	[Co III]	3d7-3d7	a2G-a2G	9/2-7/2	7.20E-03	5.76E-02	16978-17766
12.729	+	[Ni II]	3d8.(3F).4s-3d8.(3F).4s	4F-4F	7/2-5/2	2.76E-02	1.66E-01	9330-10116
12.814	++	[Ne II]	2s2.2p5-2s2.2p5	2Po-2Po	3/2-1/2	8.32E-03	1.66E-02	0-780

Results:

- forbidden [Co III] rises as predicted

-> high mass, M(Ch), is needed to avoid collisional de-excitation.

-> redistribution of energy starting after about 2 months

-> late Ni lines are (probably) there.

- [CoII] to abundant at high velocities (additional ionization source would help)
- We see Argon

- possibly Cr at 9.4 mu -> very high density

- No narrow 56Co component.

PROBING THE DIVERSITY: Why we need MIR?

SN 2014J and SN2005df have the same M(V), dm15, [Co III] but differ in the Ar distribution and, definitely, no Chromium.

Is it due to the central density ?

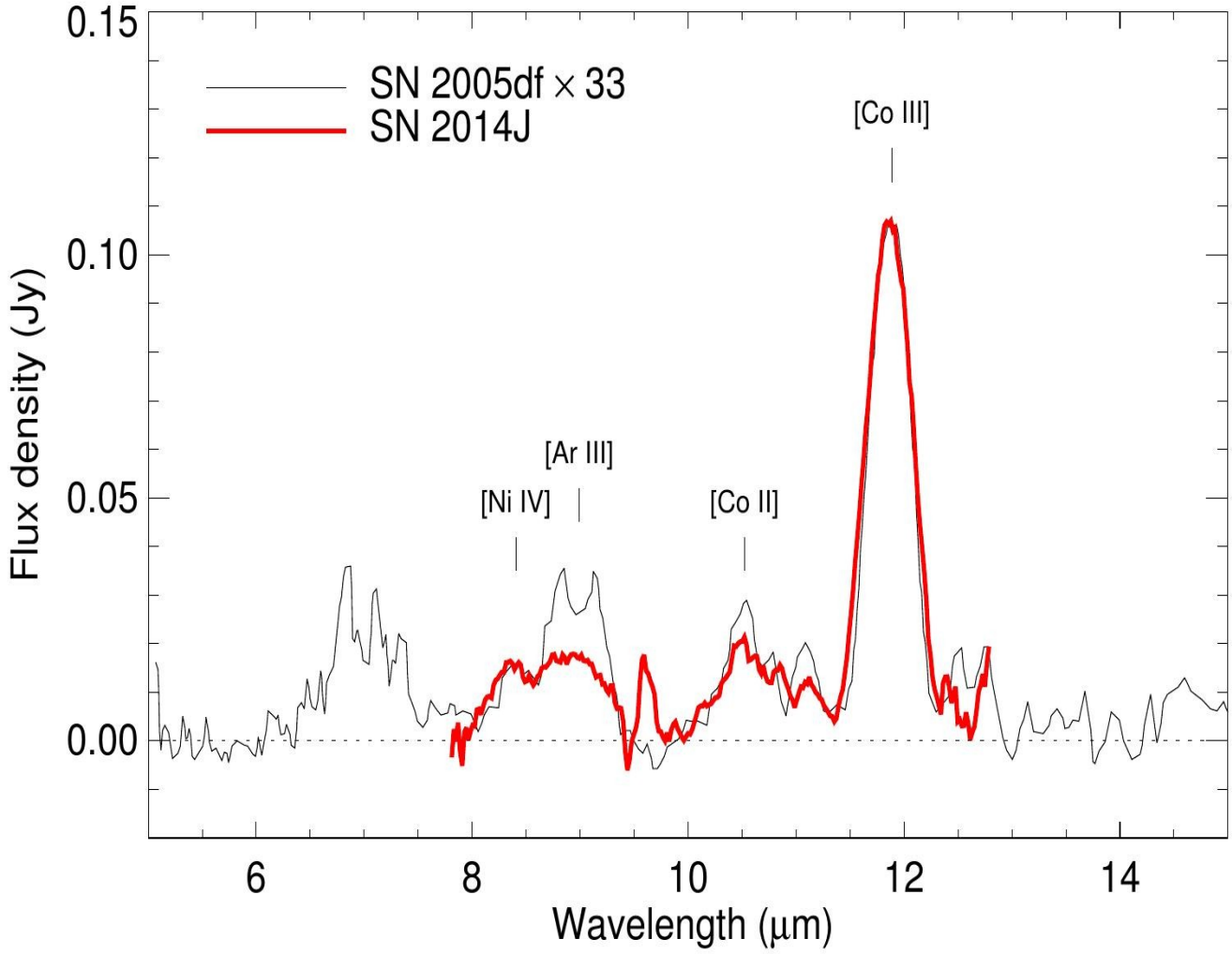

Others:

- Direct measure of photon redistribution
- [Co III] @ 11.8 mu as new standard candle ?
- magnetic fields
- mixing ...

BOLOMETRIC Light Curves

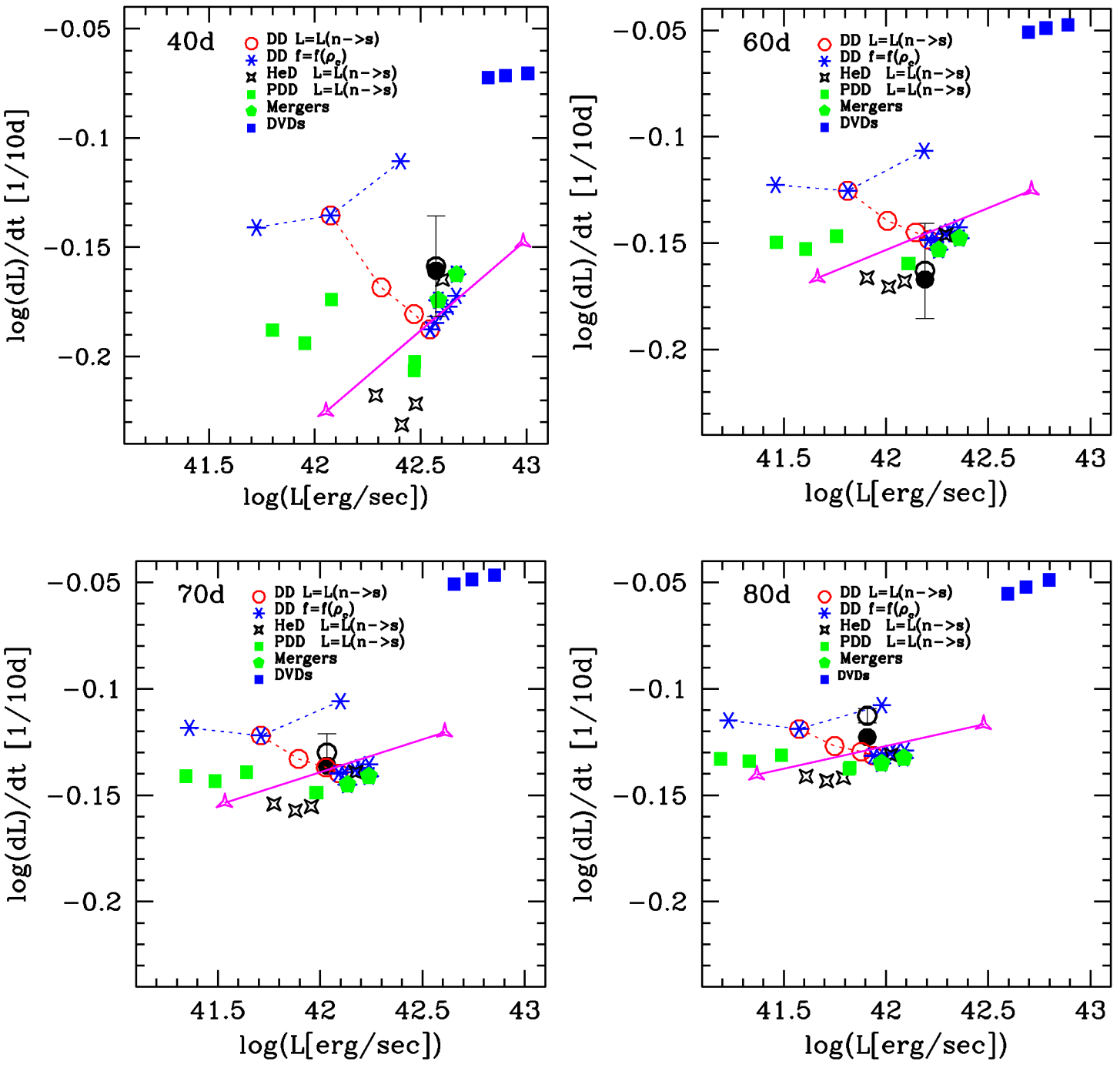

Implications of High Magnetic Fields

Smoldering phase
(Prior to Thermonuclear Runaway).

Late time Ni lines in the MIR
(SN2005df with SST, Gerardy et al. 2007)

Origin of Magnetic Fields, and its morphology.

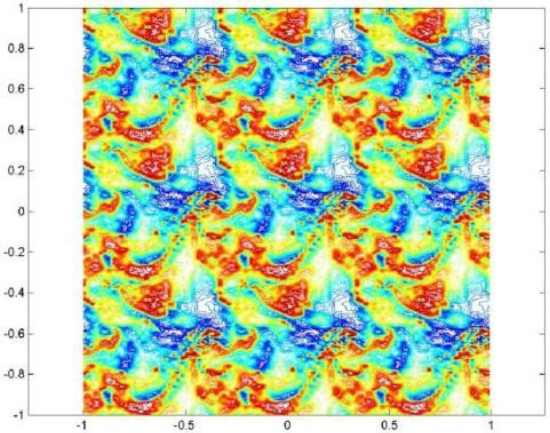

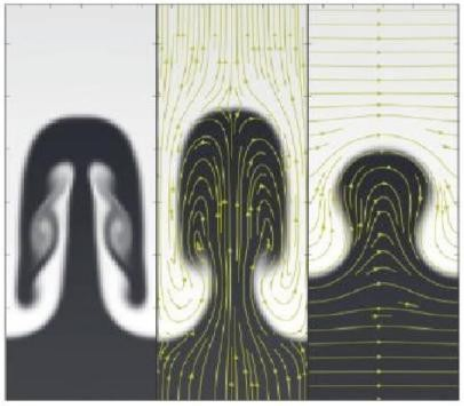

High magnetic fields in WD may be produced during the accretion phase over 1E6 to 1E8 years, during the thermonuclear runaway in a turbulent medium or by RT instabilties. On the left, we give the turbulent field used based on our calculations for the thermonuclear runaway (3). The simulations of the turbulent spectra and the influence of B on the RT instabilties (right) have been calculated using Enzo (4).

from Hoeflich, Collins, Diamond, Hengeler, Histrov, Penney (2014)

Implications of High Magnetic Fieylds (ENZO)
B. Hiskrov & D. Collins (FSU collaborators)

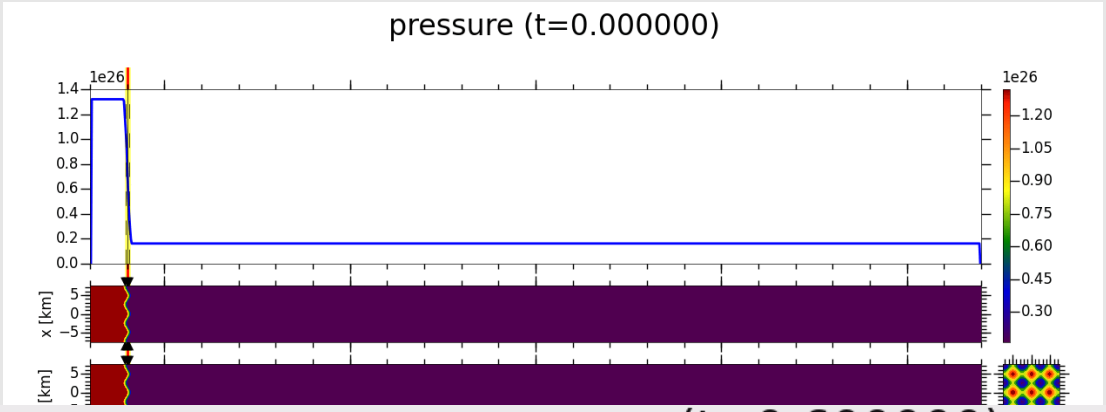

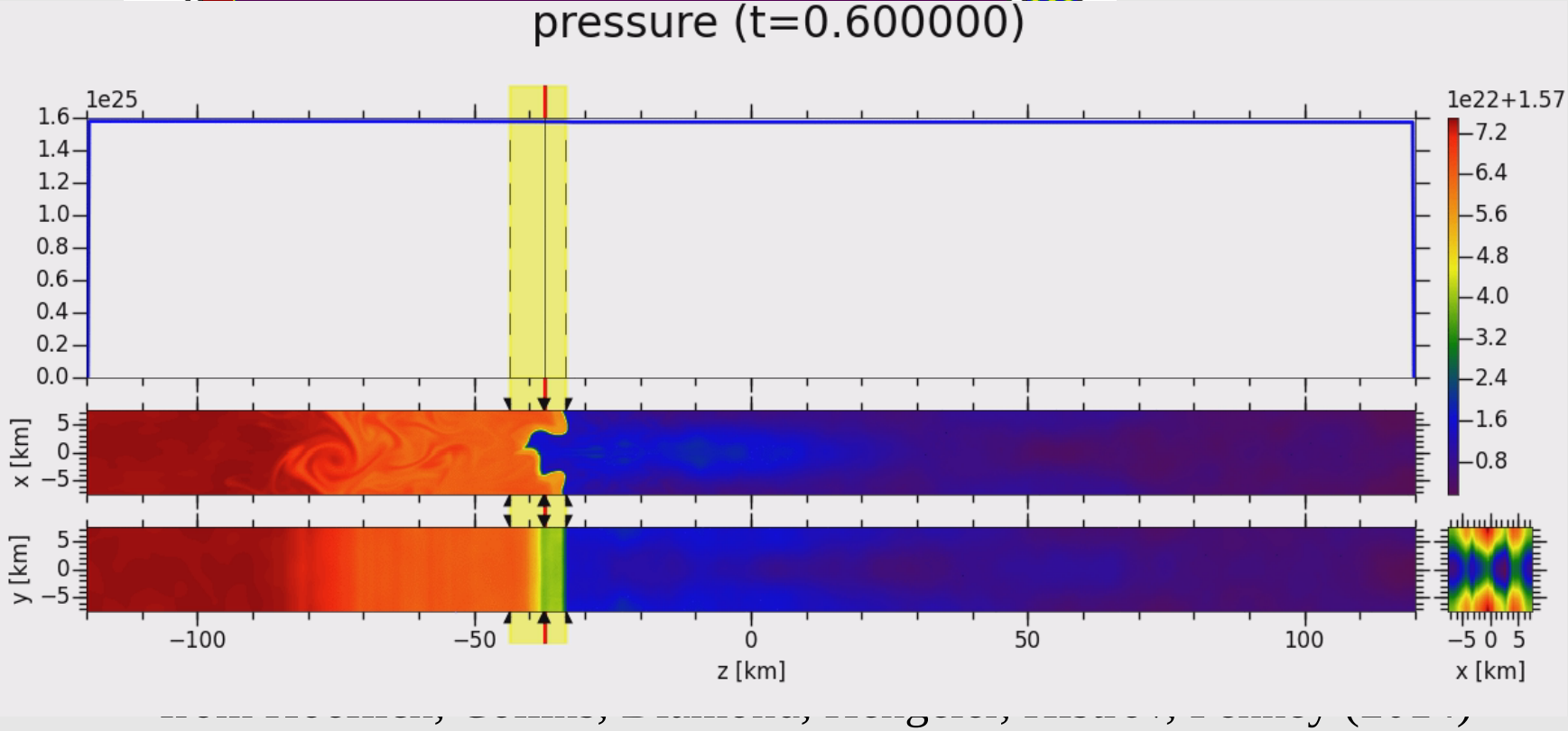

Probing B-fields by Positron Transport Effects:

(from Penney & Hoeflich 2014, Hengeler 2014, Milne 1998 to Lamour 1896)

Gamma-ray and Positron Transport effects with B-fields (5,6,7):

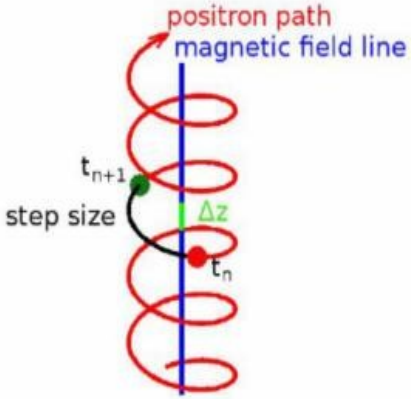

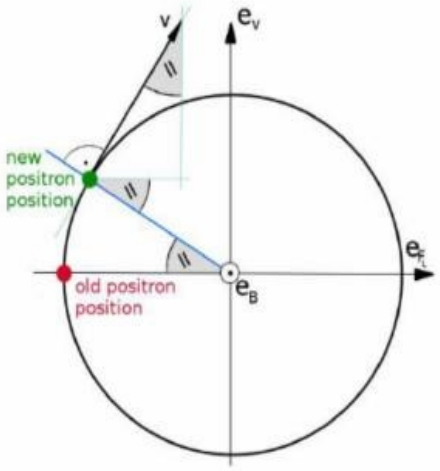

3 Cases are used for positron transport
(depending on Lamor radius R_L):

1) R_L >> R(SN) => integration along rays

2) RL < 0.001 R(SN) => positron follow B with implicit integration of path.

3) Other: formal integration of path

Positrons gyro around magnetic fields, which increases their path throughout the envelope and changes the absorption probability. Gamma-s are not effected by B.

Classical Test: Supernovae Light Curves at Late Times

(e.g. by Colgate et al. 1978, ... to Milne et al. 2001)

Can we test the magnetic fields by optical light curves ?

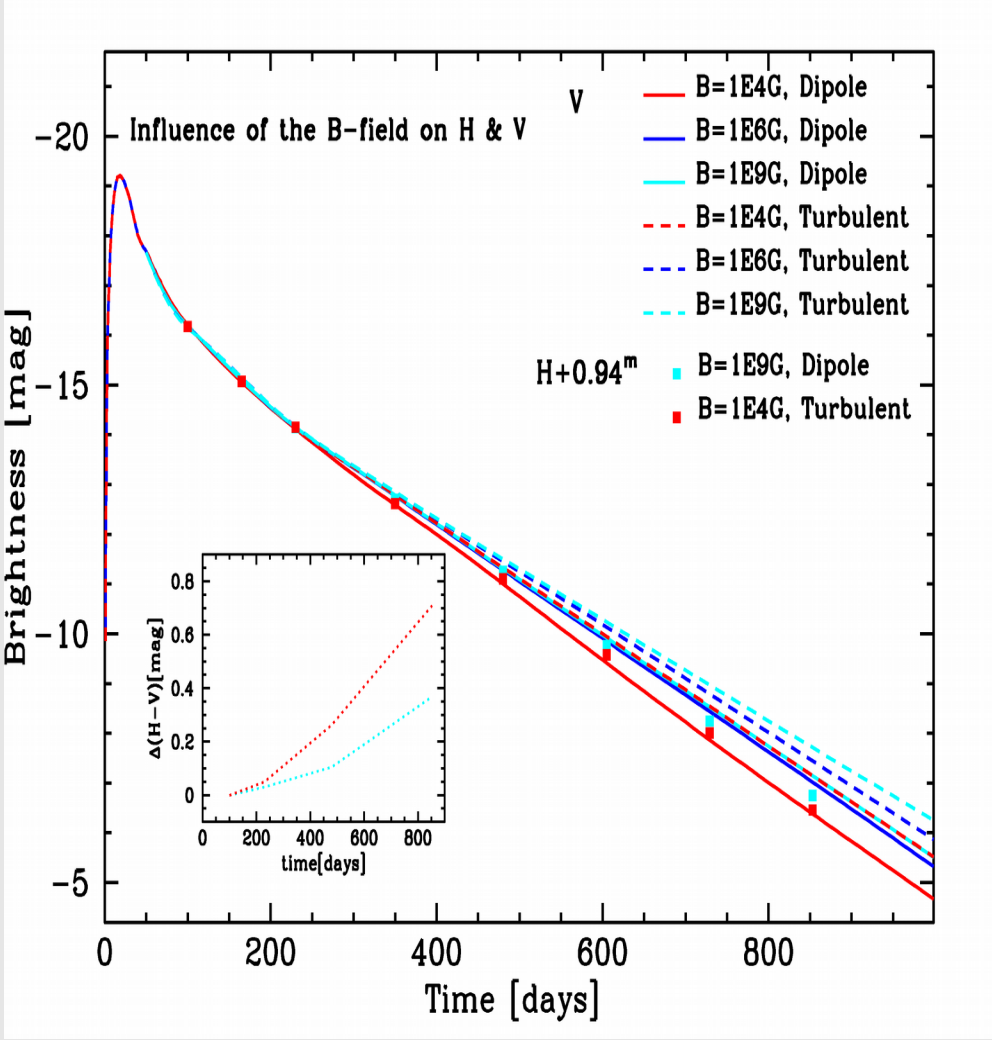

(from Penney & Hoeflich, Hengeler et al. 2014)

Result:

- Late-time LCs change up to a factor of 5 starting about 1-2 years after the explosion depending on the size and mophology of B.

Some Problemd:

- one observable but intrinsic and apparent diversity (e.g. H etal 93, H91)

Real Problem:

- H band brakes the degeneracy
- Knie measures the origin

The [Fe II] line at 1.644 mu as "Swiss-Armee Knife" @ SN 2005df

X(56Ni)= f(v)
for rho(c)

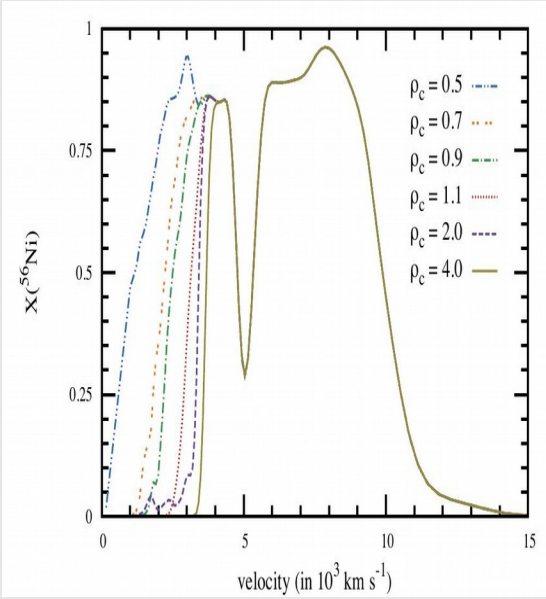

Theoretical Profiles
with Doppler-shift

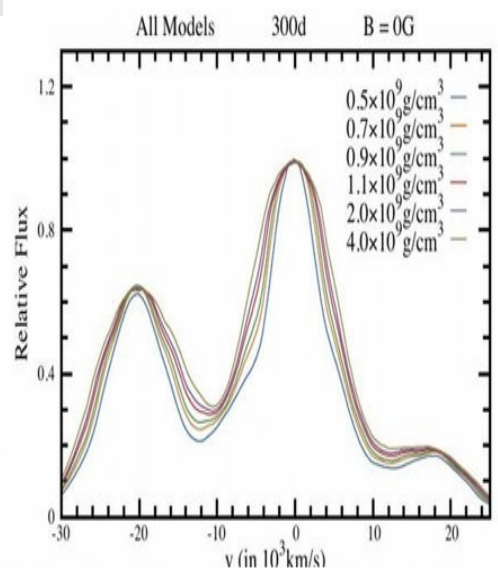

SN05df vs. Model
at day 200

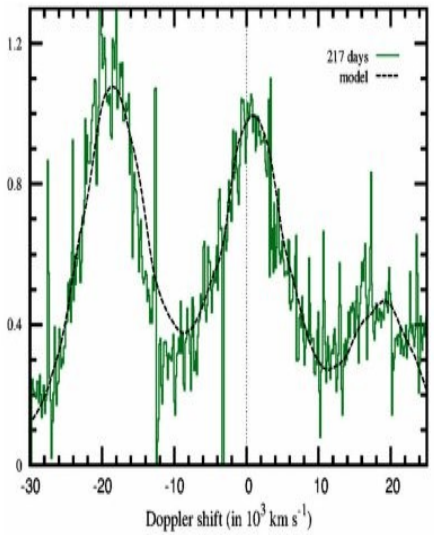

Half width=f(t)
for B=0 ,1E4 & 1E9G

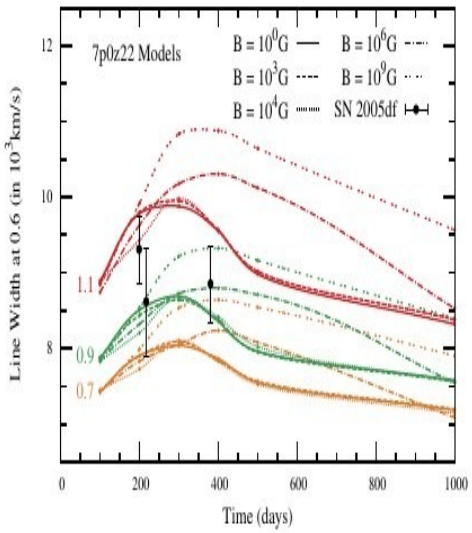

Rho(c) = log(1-M(WD)-M(Ch)

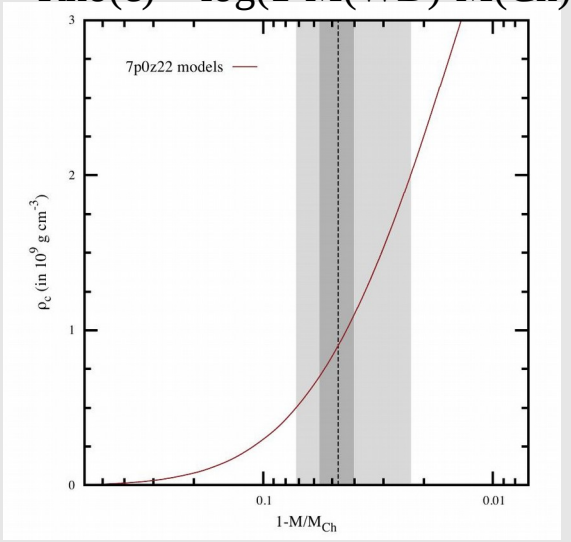

Results for SN 2005df

- M(Ch) explosion likely

- B>1E6 G best but B=0 possible (time series is needed)

- low density (almost too low for H accreter
  -> He or C (SD or DD progenitor system)

SN 2014J: A normal, unusual SNe Ia (or a twin of SN2005df)?

Same brightness as SN2005df, same decline, 0.6 Mo of 56 Ni (Diehl et al. Isern et al., Marion et al. 2014) but ...
0.06 Mo of 56Ni and narrow, non-shifted (Diehl et al. 2014ab) or blue-shifted by 18000 km/sec and broad (Isern et al. 2014) ?

varied for the counts contributed from the sky, while the instrumental background counts should

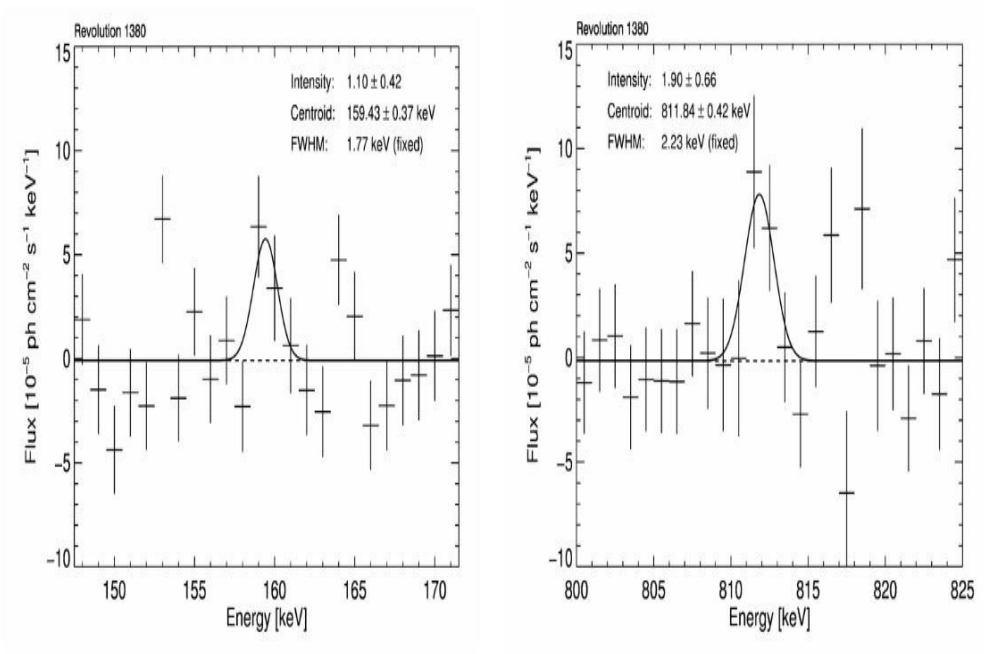

Fig.1: Gamma-ray spectra measured with SPI/INTEGRAL from SN2014J. The observed three-day interval around day 17.5 after the explosion shows the two main lines from ^{56}Ni decay. In deriving these spectra, we adopt the known position of SN2014J, and use the instrumental response and background model. Error bars are shown as 1σ. The measured intensity corresponds to an initially-synthesized ^{56}Ni mass of 0.06 $M_{\odot}$.

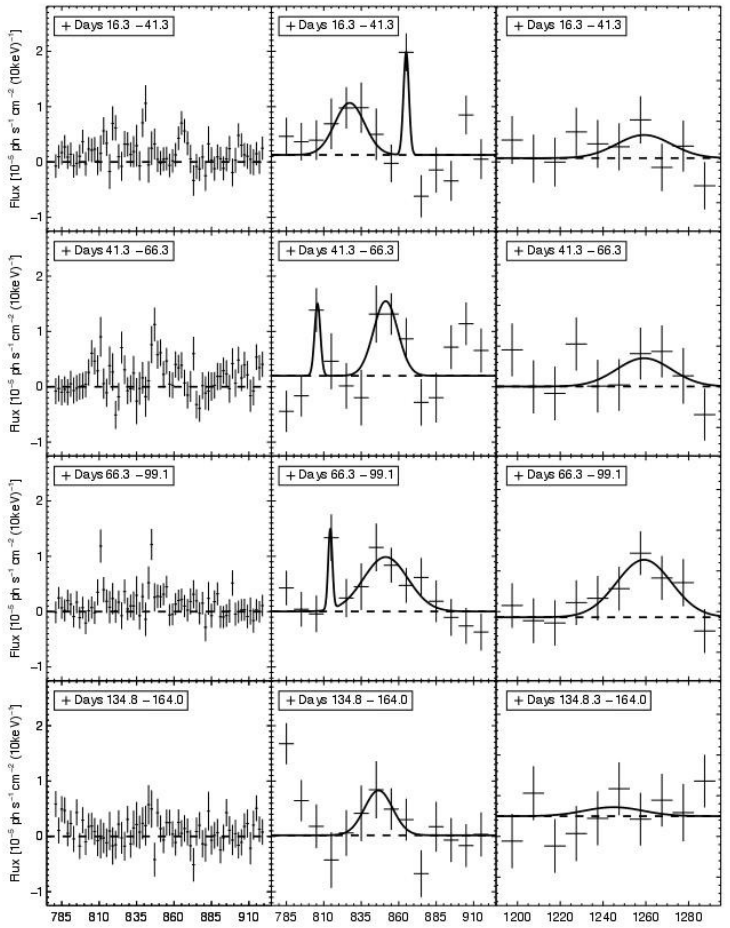

Fig. 3. SN2014J signal intensity variations for the 847 keV line (*center*) and the 1238 keV line (*right*) as seen in the four epochs of our observations, and analyzed with 10 keV energy bins. The 1238 keV fluxes have been scaled by the ^{56}Co decay branching ratio of 0.68 for equal-intensity appearance. Clear and significant emission is seen in the lower energy band (*left and center*) through a dominating broad line attributed to 847 keV emission, the emission in the high-energy band in the 1238 keV line appears consistent and weaker, as expected from the branching ratio of 0.68 (*right*). Fitted line details are discussed in the text. For the 847 keV line, in addition a high-spectral resolution analysis is shown at 2 keV energy bin width (*left*), confirming the irregular, non-broad-Gaussian features in more detail.

Summary & Future

- Double-degenerate progenitor evolution does not (!) imply M(Ch) vs. dynamical mergers !!!

- Diversity shows up in Light Curves (LSST, JWST, GMT, ELT)

(suitable for Cosmology, possible accuracy up to 0.02 m, pencil beams)

- Diversity from physical models is large

NIR and MIR spectra are absolutely needed (+ polarization)

a) To probe diversity

b) Magnetic Fields as new physics

- No first principle models !!!

Thanks

IR-Analysis of SN1999by (as followed from explosion without tuning)